

# Citrate-Assisted One-Pot Hydrothermal Preparation of Carbonated Hydroxyapatite Microspheres

Mei-li Qi <sup>1</sup>, Yanling Wu <sup>1</sup>, Cuicui Sun <sup>1</sup>, Haijun Zhang <sup>2,3</sup> and Shengkun Yao <sup>4,\*</sup><sup>1</sup> School of Civil Engineering, Shandong Jiaotong University, Jinan 250357, China<sup>2</sup> Shanghai Tenth People's Hospital, School of Medicine, Tongji University, Shanghai 200092, China<sup>3</sup> National United Engineering Laboratory for Biomedical Material Modification, Branden Industrial Park, Qihe Economic & Development Zone, Dezhou 251100, China<sup>4</sup> Shandong Provincial Engineering and Technical Center of Light Manipulations & Shandong Provincial Key Laboratory of Optics and Photonic Device, School of Physics and Electronics, Shandong Normal University, Jinan 250358, China

\* Correspondence: yaoshk@sdu.edu.cn

**Abstract:** Carbonated hydroxyapatite (CHA) microspheres have aroused wide concern in biofields because of their excellent biological and surface properties. However, the facile preparation of CHA microspheres from organic compounds, especially the microstructural transformation during synthesis, has been rarely reported. In this work, CHA microspheres with an average diameter of 2.528  $\mu\text{m}$  and a BET surface area of 51.0658  $\text{m}^2/\text{g}$  were synthesized via a one-pot hydrothermal method at 180  $^\circ\text{C}$  for 10 h by using calcium chloride, diammonium hydrogen phosphate, urea, and trisodium citrate (TSC) with a molar ratio of TSC to Ca of 1:2. The effects of hydrothermal treatment temperature and molar ratio of TSC to Ca on the morphology of the products were investigated. As a chelating agent, TSC is crucial to the formation of CHA microspheres during the hydrothermal homogeneous precipitation process. A possible mechanism of the microstructural transformation from bundle to dumbbell, dumbbell ball, and finally, microspheres regulated by TSC and urea was proposed. The CHA microspheres can be used as effective drug carriers for biomedical applications.

**Keywords:** carbonated hydroxyapatite microspheres; hydrothermal synthesis; trisodium citrate; urea



**Citation:** Qi, M.-L.; Wu, Y.; Sun, C.; Zhang, H.; Yao, S. Citrate-Assisted One-Pot Hydrothermal Preparation of Carbonated Hydroxyapatite Microspheres. *Crystals* **2023**, *13*, 551. <https://doi.org/10.3390/cryst13040551>

Academic Editor: Zhi Lin

Received: 27 February 2023

Revised: 16 March 2023

Accepted: 21 March 2023

Published: 23 March 2023



**Copyright:** © 2023 by the authors. Licensee MDPI, Basel, Switzerland. This article is an open access article distributed under the terms and conditions of the Creative Commons Attribution (CC BY) license (<https://creativecommons.org/licenses/by/4.0/>).

## 1. Introduction

Hydroxyapatite (HA) has attracted considerable attention and is widely employed in various fields, such as biomedical engineering and bone tissue engineering, because of its numerous advantages [1–3]. The effect and applications of HA particles depend substantially on their composition, morphology, and size [4,5]. Compared with other morphological types of HA, spherical HA particles exhibit a higher specific surface area and better fluidity and are promising in the fields of drug delivery, surface adsorption and protein purification [6]. Carbonated HA (CHA), whose chemical composition is similar to that of human bone, has superior bioresorption ability, osteoconductivity, and solubility [7–9]. In contrast to bone substitutes, which act as supports, CHA can be used as a bone filler to fill bone loss and strengthen bone structure [10]. Xiao et al. [11] observed faster resorption on 12 wt.% CHA microspheres which were implanted in rats compared with HA microspheres. Therefore, the design and synthesis of CHA microspheres is of great significance.

Recently, several routes have been introduced to obtain CHA microspheres, such as the spray-drying method [12], chemical etching method [13], and the widely used assistant/template-directed method [14–17]. For example, Xu et al. [18] hydrothermally prepared CHA core-shell microspheres with sodium trimetaphosphate as the phosphorus source. Wang et al. [19] fabricated hollow CHA microspheres as a slow-release vector through a biomimetic strategy. Qi et al. [20] used creatine phosphate to prepare hollow CHA microspheres through a microwave-assisted hydrothermal method. Although some

achievements have been made, some of the methods utilize unhealthy organic solvents. An environmentally friendly and convenient method to obtain CHA microspheres is still in high demand.

Citrate, a sustained-release calcium source for CHA synthesis with good biocompatibility, can regulate the nucleation, growth and hierarchical structure of particles well [21]. For example, Yang et al. [22] reported hierarchical porous HA microspheres with the help of citrate as a modifier. Urea, a homogeneous precipitator, can hydrolyze slowly to improve the pH value of the system, accompanied by a gradual increase in temperature and prolongation of time [23]. During CHA synthesis, calcium and phosphorus ions in the system are consumed slowly. In this way, the crystal nuclei formed in the early stage are still in a high environment of ion supersaturation, allowing the continual growth of CHA crystals.

In this work, we utilized trisodium citrate (TSC) as a regulating agent and urea as a homogeneous precipitator to synthesize of CHA microspheres only in one step. The effects of the hydrothermal treatment temperature and molar ratio of TSC/Ca gradients on the morphology of the CHA microspheres were investigated. The potential formation mechanism of CHA microspheres was systematically discussed. Compared with other routes to obtain CHA microspheres, the hydrothermal homogeneous precipitation method involves one step without a subsequent sintering process and is environmentally friendly since no toxic solvent is used. Moreover, the CHA microspheres exhibit a relatively large surface area, which contributes to drug loading and release.

## 2. Materials and Methods

### 2.1. Materials

Chemical reagents including anhydrous calcium chloride ( $\text{CaCl}_2$ , AR), diammonium hydrogen phosphate ( $(\text{NH}_4)_2\text{HPO}_4$ , AR), nitric acid ( $\text{HNO}_3$ , AR), TSC (AR), urea ( $\text{CO}(\text{NH}_2)_2$ , AR), and nitric acid solution ( $\text{HNO}_3$ , AR) were received from Sinopharm Chemical Reagent Company Limited of China (Shanghai, China) and used without any other purification.

### 2.2. Sample Preparation

CHA products were obtained using a one-step hydrothermal homogeneous precipitation method. First, aqueous solutions of  $(\text{NH}_4)_2\text{HPO}_4$  (0.06 mol/L),  $\text{CaCl}_2$  aqueous solution (0.01 mol/L) and urea (1 mol/L) were prepared and mixed together under magnetic stirring. Secondly, the initial solution pH value was adjusted to 3 by a dilute  $\text{HNO}_3$  solution. When the solution became clear and uniform, TSC was added while the TSC/Ca molar ratio was kept at 1 and 2. After that, the solutions were moved to Teflon-lined hydrothermal reactors, followed by treatment at 150 °C, 160 °C, and 180 °C for 10 h. Finally, the obtained resultants were washed centrifugally with deionized water and ethanol thoroughly and dried to obtain a white powder.

### 2.3. Characterization

The phase composition and functional groups of the powder were identified by X-ray diffraction (XRD, Bruker D8 Advance,  $\text{CuK}\alpha$  radiation,  $\lambda = 1.5418 \text{ \AA}$ ) and Fourier transform infrared spectroscopy (FTIR, Nicolet IS50, Holland). The morphology and microstructure study of the powder was conducted under a field scanning electron microscope (FE-SEM, JSM-7610F, Tokyo, Japan) and high-resolution transmission electron microscope (HRTEM, JEM2100Plus, Tokyo, Japan). The powder was sputter-coated with gold before the FE-SEM tests due to their nonconductivity. A particle size analyzer with laser diffraction (Mastersizer 2000, Malvern, England) was utilized to evaluate the particle size distribution (PSD) and mean particle size. To improve the dispersion, the powder was treated ultrasonically in anhydrous ethanol and deionized water for 10 min before TEM and PSD tests. The Brunauer–Emmett–Teller (BET) surface area as well as Barrett–Joyner–Halenda (BJH) pore diameter were obtained by a Micromeritics ASAP 2460 instrument (nitrogen adsorption–desorption isotherms).

### 3. Results

This section may be divided by subheadings. It should provide a concise and precise description of the experimental results, their interpretation, as well as the experimental conclusions that can be drawn.

#### 3.1. Phase and Functional Group Analysis

XRD patterns and FTIR spectra of the powder samples under different hydrothermal reaction temperatures and molar ratios of TSC/Ca are displayed in Figure 1 to detect their phase composition as well as functional groups. As is shown in the XRD patterns (Figure 1a), all the products were identified to HA phase compared to the standard HA in the purple bar chart below (JCPDS 09-0432). In addition, the diffraction peak intensity became stronger as the hydrothermal temperature increased from 120 °C to 180 °C at a 1:1 TSC/Ca molar ratio, indicating the increase in the crystallinity. Changing the molar ratio of TSC/Ca did not change the phase of the products; however, with a decrease in the TSC/Ca molar ratio, the crystallinity degree of the powder sample decreased.

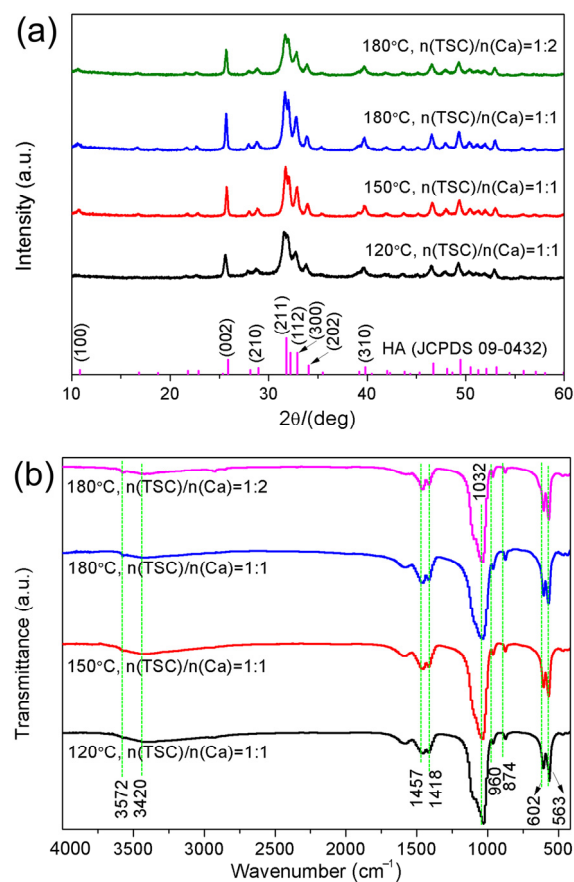


**Figure 1.** XRD patterns (a) and FTIR spectra (b) of the powder prepared by TSC and urea under different hydrothermal reaction temperatures and molar ratios of TSC/Ca.

The functional groups of the products further support the above results since all the FTIR spectra have similar patterns (Figure 1b). The broad peaks at 3420 and 3572  $\text{cm}^{-1}$  were ascribed to water molecules and OH- groups, respectively [13,24]. The peaks at 960, 602 and 563  $\text{cm}^{-1}$  were attributed to the  $\text{PO}_4^{3-}$  group [25]. The three IR bands at 1457, 1418, and 874  $\text{cm}^{-1}$  were the characteristic bands of  $\text{CO}_3^{2-}$  produced by the hydrolysis of urea above 80 °C, indicating that  $\text{CO}_3^{2-}$  ions replace some  $\text{PO}_4^{3-}$  ions and form type B-type HA [26]. These results further prove that the prepared HA products are CHA, similar to the inorganic components in natural bone.

### 3.2. Microstructural Characterization

The morphological evolution of the CHA products obtained under different hydrothermal reaction temperatures and molar ratios of TSC/Ca were observed by SEM and TEM (Figures 2 and 3). It is clear that bundle CHA crystals with a length of approximately 1  $\mu\text{m}$  first formed and then grew into larger dumbbells as the hydrothermal temperature increased from 120  $^{\circ}\text{C}$  to 150  $^{\circ}\text{C}$  (Figures 2a,b and 3a,b). When the hydrothermal temperature increased to 180  $^{\circ}\text{C}$ , the dumbbells became dense, and dumbbell balls with a diameter of 3–4  $\mu\text{m}$  appeared (Figure 2c). However, when the molar ratio of TSC/Ca changed to 1:2, the CHA dumbbell balls continued to grow into CHA microspheres (Figures 2d and 3c).

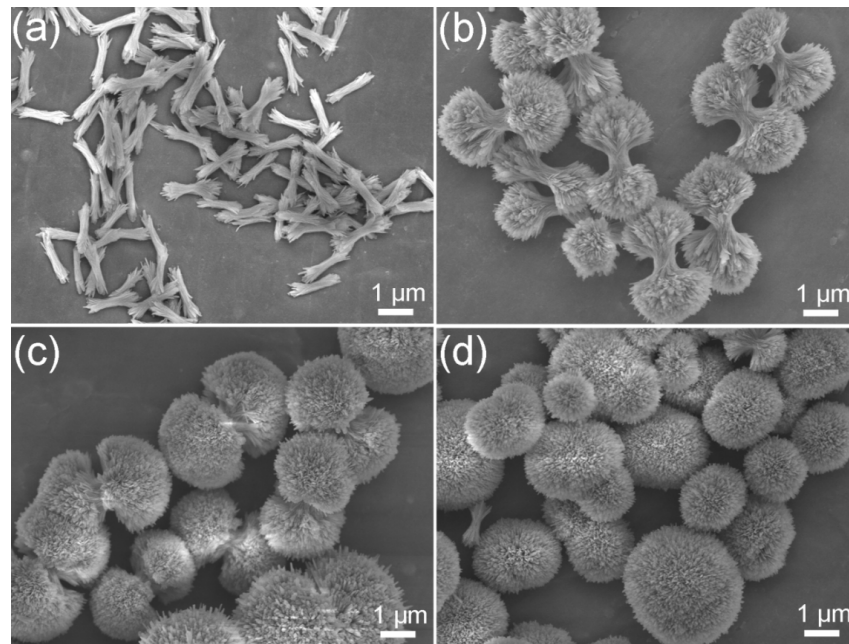


**Figure 2.** FE-SEM images of the CHA products synthesized by TSC and urea under different hydrothermal reaction temperatures and molar ratios of TSC/Ca. (a) 120  $^{\circ}\text{C}$ , (b) 150  $^{\circ}\text{C}$ , and (c) 180  $^{\circ}\text{C}$  with  $n(\text{TSC})/n(\text{Ca}) = 1$ , and (d) 180  $^{\circ}\text{C}$  with  $n(\text{TSC})/n(\text{Ca}) = 1:2$ .

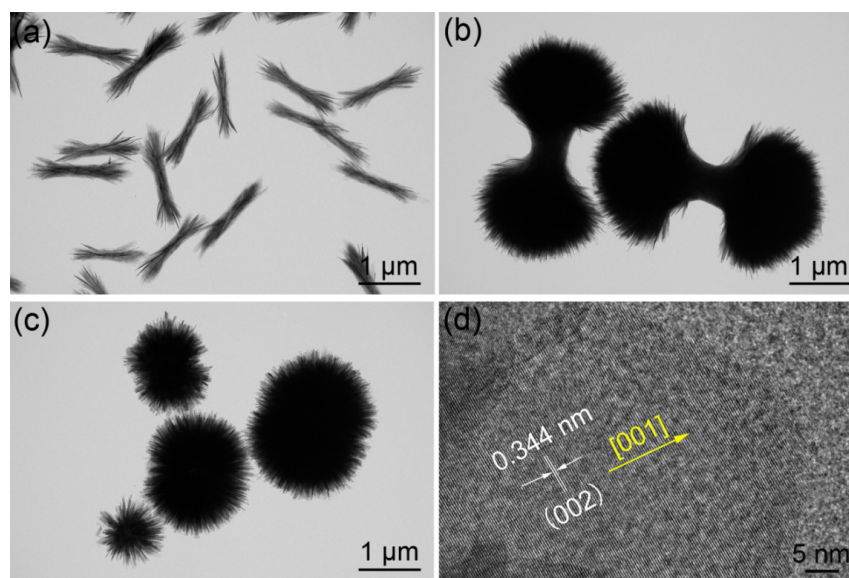


**Figure 3.** TEM images of the CHA products hydrothermally synthesized by TSC and urea at (a) 120  $^{\circ}\text{C}$  with  $n(\text{TSC})/n(\text{Ca}) = 1:1$ , (b) 150  $^{\circ}\text{C}$  with  $n(\text{TSC})/n(\text{Ca}) = 1:1$ , (c) 180  $^{\circ}\text{C}$  with  $n(\text{TSC})/n(\text{Ca}) = 1:2$ , and (d) an HRTEM image of (c).

The HRTEM image of the CHA microspheres with a 1:2 TSC/Ca molar ratio (Figure 3d) shows a lattice fringe with an interplanar spacing of 0.344 nm, which corresponded to the (002) plane of crystalline HA. This result is consistent with the abovementioned XRD results (Figure 1d).

### 3.3. Particle Dispersity and Specific Surface Area Analysis

Particle size distribution and pore structures have a very important influence on the properties of CHA microspheres. From the particle size distribution curve (Figure 4a), it can be seen that most of the CHA microspheres ranged in size from 0.5 to 10  $\mu\text{m}$ . Moreover, the mean particle size of the microspheres was 2.528  $\mu\text{m}$ . As determined via the BET method, the specific surface area of the CHA microspheres was 51.0658  $\text{m}^2/\text{g}$ . The pore structure of the CHA microspheres was determined by the  $\text{N}_2$  adsorption–desorption isotherm and its corresponding pore distribution distributions (Figure 4b,c). Based on the International Union of Pure and Applied Chemistry, CHA microspheres can be classified as type IV with a type H3 hysteresis loop, demonstrating a prominent mesoporous structure with good pore accessibility [27]. While the majority of the pore volume is composed of mesopores, most of the pores are 0–40 nm in size. Based on the desorption curve of the nitrogen isotherm, the mean pore diameter of CHA microspheres is determined to be 17.1623 nm, as calculated by the BJH method. The relatively large specific surface area and nanoporous structure of the CHA microspheres offer ideal nanoscale channels as well as physical space to load and deliver drugs, and therefore, are favorable for drug-delivery applications.

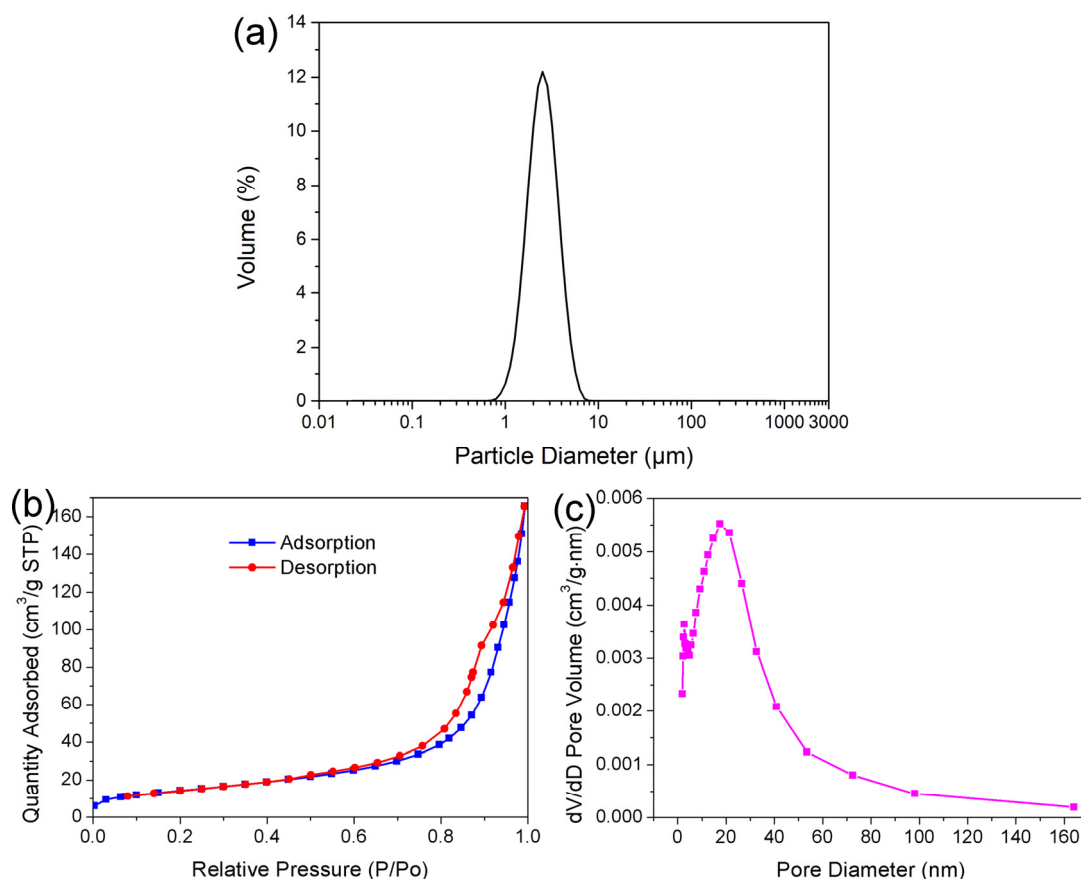


**Figure 4.** Particle size distributions (a), nitrogen adsorption–desorption isotherms (b), and pore size distributions (c) of the HA microspheres prepared with a 1:2 TSC/Ca molar ratio.

### 3.4. Formation Mechanism of CHA Microspheres Regulated by TSC and Urea

To demonstrate the formation of CHA microspheres in a hydrothermal homogeneous precipitation with the regulation of TSC and urea, a possible formation mechanism is

proposed in Figure 5. At the early stage, citrate combined with  $\text{Ca}^{2+}$  ions in the reactive system to form calcium citrate, which is a soluble complex, hindering the direct formation of CHA precipitates. The stability of calcium citrate increases with elevated solution pH. Urea hydrolyzes slowly to produce  $\text{OH}^-$  when the hydrothermal temperature reaches  $80\text{ }^\circ\text{C}$ . The hydrolysis as well as the supersaturation of the whole reaction system can be accelerated with increasing temperature [20]. When the supersaturation reaches a certain value,  $\text{Ca}^{2+}$  ions can be slowly released, accompanied by the hydrolysis of calcium citrate. In this way, the nucleation and growth of CHA crystals is regulated. Moreover,  $\text{CO}_3^{2-}$  is formed upon hydrolysis of urea. In the solution,  $\text{PO}_4^{3-}$ ,  $\text{OH}^-$ , and  $\text{CO}_3^{2-}$  ions are combined with free  $\text{Ca}^{2+}$  ions. A plate-like CHA crystal nucleus starts to form and gather together to grow into bundle-like crystallites. At the early stage, a rather high supersaturation of the solution leads to a great deal of bundle-like CHA crystallites. To reduce the overall surface energy, these bundles grow larger and self-assemble into each other to form dumbbell clusters when the hydrothermal temperature increases to  $150\text{ }^\circ\text{C}$ . With a further increase in the hydrothermal temperature to  $180\text{ }^\circ\text{C}$ , dumbbell clusters grow into dumbbell balls. When the molar ratio was changed to 1:2, TSC was fully complexed with  $\text{Ca}^{2+}$  ions in the system; thus,  $\text{Ca}^{2+}$  has an increased chance to react with TSC, and finally, regular CHA microspheres are obtained. Therefore, according to the above analysis, a hydrothermal reaction temperature of  $180\text{ }^\circ\text{C}$  and TSC/Ca molar ratio of 1:2 are conducive to the formation of CHA microspheres.

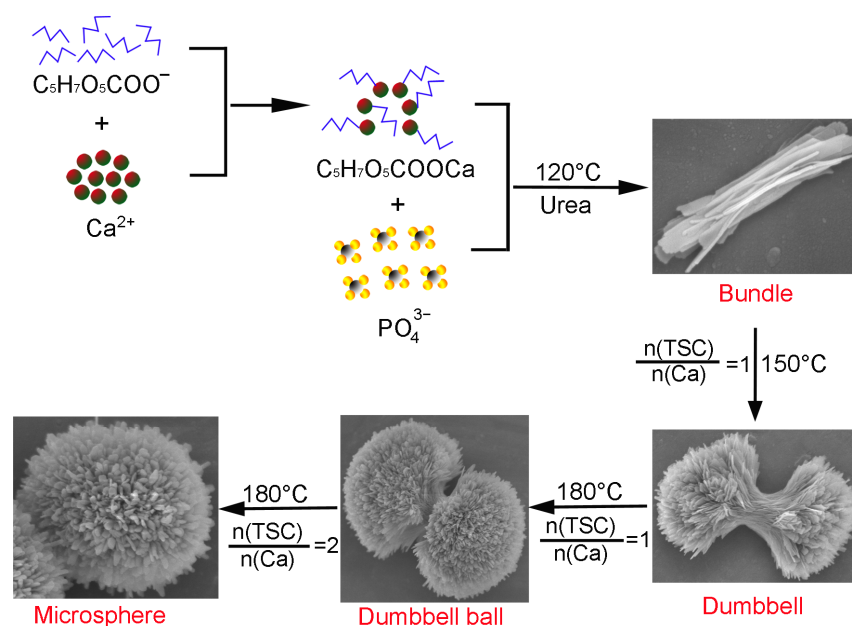


**Figure 5.** Formation mechanism of porous HA microspheres by TSC and urea via a hydrothermal route.

There are two key factors accounting for the formation of CHA microspheres. On the one hand, the increase in temperature changes the activation energy during each process of crystal growth, accelerates the release of  $\text{Ca}^{2+}$  ions, increases the probability of binding with  $\text{PO}_4^{3-}$  ions and improves the reaction rate to obtain CHA products. The rising temperature also accelerates the dissolution process, changes the solubility of the solute, increases the concentration of  $\text{Ca}^{2+}$  ions released in the solution and the concentration of  $\text{OH}^-$  ions produced by urea hydrolysis, and increases the supersaturation ratio of the solution. When the saturation ratio required for nucleation is reached, the crystal nuclei formed in the early stage are deposited under the nutritional conditions of growth. On the other hand, an appropriate molar ratio of TSC/Ca promotes the chemical reaction in the forward direction. The driving force increases as the reaction goes on; thus, the interface produces continuous growth, and the CHA crystals start to grow into microspheres. Compared to other routes

to synthesize CHA microspheres, this process is advantageous because no toxic organic solvents are utilized, and it is a one-step process without subsequent sintering. Moreover, the obtained CHA microspheres exhibit a large surface area, making them good candidates for drug loading and release. Both in vitro and in vivo experiments need to be performed to examine the biological properties of CHA microspheres in the future.

#### 4. Conclusions

In this work, CHA microspheres with an average diameter of 2.528  $\mu\text{m}$  and a BET surface area of 51.0658  $\text{m}^2/\text{g}$  were successfully obtained by TSC via a one-pot hydrothermal method. The experimental results showed that hydrothermal treatment temperature and molar ratio of TSC/Ca are the key factors to control the morphology of the CHA products from bundles to dumbbells, dumbbell balls and finally microspheres. Well-developed CHA microspheres with uniform morphology were obtained at 180  $^{\circ}\text{C}$  for 10 h with a TSC/Ca molar ratio of 1:2. Moreover, a possible mechanism for the formation of CHA microspheres was proposed. Such CHA microspheres with a relatively big BET surface area are expected to be used as drug carriers, separation media and filling materials.

**Author Contributions:** Data curation, C.S.; funding acquisition, M.-I.Q.; investigation, Y.W.; resources, H.Z.; supervision, S.Y.; writing—original draft preparation, M.-I.Q.; writing—review and editing, S.Y. All authors have read and agreed to the published version of the manuscript.

**Funding:** This research was funded by Young Talent of Lifting Engineering for Science and Technology in Shandong, China (Award No. SDAST2021qt05), the Natural Science Foundation of Shandong Province (Award Nos. ZR2020QE070 and ZR2020QA076) and the National Natural Science Foundation of China (Award No. 12004227).

**Data Availability Statement:** Data is contained within the article.

**Conflicts of Interest:** The authors declare no conflict of interest.

#### References

1. Roy, D.M.; Linnehan, S.K. Hydroxyapatite formed from coral skeletal carbonate by hydrothermal exchange. *Nature* **1974**, *247*, 220–222. [[CrossRef](#)]
2. Tien Lam, N.; Minh Quan, V.; Boonrungsiman, S.; Sukyai, P. Effectiveness of bio-dispersant in homogenizing hydroxyapatite for proliferation and differentiation of osteoblast. *J. Colloid Interface Sci.* **2022**, *611*, 491–502. [[CrossRef](#)] [[PubMed](#)]
3. Zhang, M.; Qi, M.-L.; Yuan, K.; Liu, H.; Ren, J.; Liu, A.; Yao, S.; Guo, X.; Li, X.; Zhang, H. Integrated porous polyetheretherketone implants for treating skull defect. *J. Mater. Res. Technol.* **2023**, *22*, 728–734. [[CrossRef](#)]
4. Lin, K.; Wu, C.; Chang, J. Advances in synthesis of calcium phosphate crystals with controlled size and shape. *Acta Biomater.* **2014**, *10*, 4071–4102. [[CrossRef](#)]
5. Wang, Y.-C.; Xu, W.-L.; Lu, Y.-P.; Xu, W.-H.; Yin, H.; Xiao, G.-Y. Investigation of nature of starting materials on the construction of hydroxyapatite 1D/3D morphologies. *Mater. Sci. Eng. C* **2020**, *108*, 110408. [[CrossRef](#)]
6. Qi, M.-L.; Qi, J.; Xiao, G.-Y.; Zhang, K.-Y.; Lu, C.-Y.; Lu, Y.-P. One-step hydrothermal synthesis of carbonated hydroxyapatite porous microspheres with a large and uniform size regulated by l-glutamic acid. *CrystEngComm* **2016**, *18*, 5876–5884. [[CrossRef](#)]
7. Landi, E.; Celotti, G.; Logroscino, G.; Tampieri, A. Carbonated hydroxyapatite as bone substitute. *J. Eur. Ceram. Soc.* **2003**, *23*, 2931–2937. [[CrossRef](#)]
8. Benataya, K.; Lakrat, M.; Elansari, L.L.; Mejdoubi, E. Synthesis of B-type carbonated hydroxyapatite by a new dissolution-precipitation method. *Mater. Today Proc.* **2020**, *31*, S83–S88. [[CrossRef](#)]
9. Germaini, M.-M.; Detsch, R.; Grünwald, A.; Magnaudeix, A.; Lalloué, F.; Boccacini, A.R.; Champion, E. Osteoblast and osteoclast responses to A/B type carbonate-substituted hydroxyapatite ceramics for bone regeneration. *Biomed. Mater.* **2017**, *12*, 035008. [[CrossRef](#)]
10. Falacho, R.; Palma, P.; Marques, J.; Figueiredo, M.; Caramelo, F.; Dias, I.; Viegas, C.; Guerra, F. Collagenated porcine heterologous bone grafts: Histomorphometric evaluation of bone formation using different physical forms in a rabbit cancellous bone model. *Molecules* **2021**, *26*, 1339. [[CrossRef](#)]
11. Xiao, W.; Sonny Bal, B.; Rahaman, M.N. Preparation of resorbable carbonate-substituted hollow hydroxyapatite microspheres and their evaluation in osseous defects in vivo. *Mater. Sci. Eng. C* **2016**, *60*, 324–332. [[CrossRef](#)]
12. Sun, R.; Lu, Y.; Chen, K. Preparation and characterization of hollow hydroxyapatite microspheres by spray drying method. *Mater. Sci. Eng. C* **2009**, *29*, 1088–1092. [[CrossRef](#)]
13. Guo, Y.-J.; Wang, Y.-Y.; Chen, T.; Wei, Y.-T.; Chu, L.-F. Hollow carbonated hydroxyapatite microspheres with mesoporous structure: Hydrothermal fabrication and drug delivery property. *Mater. Sci. Eng. C* **2013**, *33*, 3166–3172. [[CrossRef](#)] [[PubMed](#)]

14. Jiang, S.-D.; Yao, Q.-Z.; Zhou, G.-T.; Fu, S.-Q. Fabrication of hydroxyapatite hierarchical hollow microspheres and potential application in water treatment. *J. Phys. Chem. C* **2012**, *116*, 4484–4492. [[CrossRef](#)]
15. Lin, K.; Liu, P.; Wei, L.; Zou, Z.; Zhang, W.; Qian, Y.; Shen, Y.; Chang, J. Strontium substituted hydroxyapatite porous microspheres: Surfactant-free hydrothermal synthesis, enhanced biological response and sustained drug release. *Chem. Eng. J.* **2013**, *222*, 49–59. [[CrossRef](#)]
16. Xiao, W.; Gao, H.; Qu, M.; Liu, X.; Zhang, J.; Li, H.; Yang, X.; Li, B.; Liao, X. Rapid microwave synthesis of hydroxyapatite phosphate microspheres with hierarchical porous structure. *Ceram. Int.* **2018**, *44*, 6144–6151. [[CrossRef](#)]
17. Qi, M.-L.; Yao, S.; Liu, X.-C.; Wang, X.; Cui, F. Nanosheet-assembled carbonated hydroxyapatite microspheres prepared by an EDTA-assisted hydrothermal homogeneous precipitation route. *CrystEngComm* **2020**, *22*, 2884–2888. [[CrossRef](#)]
18. Xu, W.-L.; Ci, L.-J.; Qi, M.-L.; Xiao, G.-Y.; Chen, X.; Xu, W.-H.; Lu, Y.-P. Sr<sup>2+</sup>-dependent microstructure regulation of biodegradable Sr-doped hydroxyapatite microspheres with interconnected porosity for sustained drug delivery. *Ceram. Int.* **2023**. *in Press*. [[CrossRef](#)]
19. Wang, K.; Wang, Y.; Zhao, X.; Li, Y.; Yang, T.; Zhang, X.; Wu, X. Sustained release of simvastatin from hollow carbonated hydroxyapatite microspheres prepared by aspartic acid and sodium dodecyl sulfate. *Mater. Sci. Eng. C* **2017**, *75*, 565–571. [[CrossRef](#)]
20. Qi, C.; Zhu, Y.; Lu, B.-Q.; Zhao, X.-Y.; Zhao, J.; Chen, F.; Wu, J. Hydroxyapatite hierarchically nanostructured porous hollow microspheres: Rapid, sustainable microwave-hydrothermal synthesis by using creatine phosphate as an organic phosphorus source and application in drug delivery and protein adsorption. *Chem. A Eur. J.* **2013**, *19*, 5332–5341. [[CrossRef](#)]
21. Yang, H.; Hao, L.; Du, C.; Wang, Y. A systematic examination of the morphology of hydroxyapatite in the presence of citrate. *RSC Adv.* **2013**, *3*, 23184–23189. [[CrossRef](#)]
22. Yang, H.; Hao, L.; Zhao, N.; Du, C.; Wang, Y. Hierarchical porous hydroxyapatite microsphere as drug delivery carrier. *CrystEngComm* **2013**, *15*, 5760–5763. [[CrossRef](#)]
23. Yang, Y.; Wu, Q.; Wang, M.; Long, J.; Mao, Z.; Chen, X. Hydrothermal synthesis of hydroxyapatite with different morphologies: Influence of supersaturation of the reaction system. *Cryst. Growth Des.* **2014**, *14*, 4864–4871. [[CrossRef](#)]
24. Fowler, B.O. Infrared studies of apatites. I. Vibrational assignments for calcium, strontium, and barium hydroxyapatites utilizing isotopic substitution. *Inorg. Chem.* **1974**, *13*, 194–207. [[CrossRef](#)]
25. Sun, R.; Yang, L.; Zhang, Y.; Chu, F.; Wang, G.; Lv, Y.; Chen, K. Novel synthesis of AB-type carbonated hydroxyapatite hierarchical microstructures with sustained drug delivery properties. *CrystEngComm* **2016**, *18*, 8030–8037. [[CrossRef](#)]
26. Vignoles, M.; Bonel, G.; Holcomb, D.W.; Young, R.A. Influence of preparation conditions on the composition of type B carbonated hydroxyapatite and on the localization of the carbonate ions. *Calcif. Tissue Int.* **1988**, *43*, 33–40. [[CrossRef](#)]
27. Mei, F.; Yao, S.; Xu, W.-L.; Wu, Y.; Wang, Y.; Qi, M.-L. Facile and simple synthesis of silver-doped hydroxyapatite porous microspheres with good sphericity. *Micro Nano Lett.* **2021**, *16*, 425–431. [[CrossRef](#)]

**Disclaimer/Publisher’s Note:** The statements, opinions and data contained in all publications are solely those of the individual author(s) and contributor(s) and not of MDPI and/or the editor(s). MDPI and/or the editor(s) disclaim responsibility for any injury to people or property resulting from any ideas, methods, instructions or products referred to in the content.